ARCHIVES OF ACOUSTICS
8, 3, 185-204 (1983)

FOCUSING OF AN ULTRASONIC BEAM BY MEANS OF A PIEZOELECTRIC ANNULAR ARRAY

T. WASZCZUK, T. KUJAWSKA

Department of Ultrasound, Institute of Fundamental Technological Research, Polish Academy of Sciences
(00-049 Warsaw, ul. Świętokrzyska 21)

J. C. SOMER

University of Limburg, Biophysics Department
(6200 MD Maastricht, Holland)

The lateral resolution of ultrasonographs for the investigation of the internal structures of the body depends on the diameter of the ultrasonic beam. A decrease in the diameter of the beam can be achieved by the use of multi-element annular ultrasonic probe controlled by the electronic system described in the present paper. This paper also presents a method for the calculation of the distribution of the radiated acoustic field and two experimental methods which permit the measurement of the field distribution, with focusing during transmission only. The analytical results were compared with the experimental results obtained by two measurement methods. This comparison indicates that over the major part of the range there is agreement between the analytical and experimental results. Some differences between them occur mainly at the ends of zone 2 (focal point 60 mm) and in zone 4 (focal point 110 mm).

1. Introduction

One of the fundamental methods of investigation in ultrasonic medical diagnosis is *B*-mode echography. In this mode the reflected echoes, which correspond to the distribution of anatomical structures of the body, are shown as bright points on the screen of the CRT. The brightness and diameter of these points depend on the amplitude of the echoes and the diameter of the electron beam of the CRT. In good quality CRT, echoes with mean amplitude are shown as points of 0.5 mm diameter [4]. This diameter can be taken as the criterion in *B*-mode ultrasonographs for the investigation of the internal structures, in order that a good resolution may be achieved.

The resolution of the ultrasonograph is defined by the longitudinal and lateral resolution of the ultrasonic probe, the accuracy of deflection and focusing of the electron beam in the CRT, the mechanical stability of the system which transforms the motion of the probe into the motion of the time base on the screen and by variations in the velocity of the ultrasonic beam in investigated structures. In addition to variations in the velocity of the ultrasonic beam in the structures, other parameters result from the design and accomplishment of the equipment.

In the present state of ultrasonic technology the most negative effect on the resolution of the ultrasonograph is exerted by the lateral resolution of the ultrasonic probe. The other parameters permit the achievement of the resolution which results from the size of a spot on the CRT screen.

The lateral resolution is defined as the minimum distance between two elements reflecting the ultrasonic beam. The signals reflected from these elements should be displayed as two independent echoes on the screen of the CRT. The lateral resolution of the ultrasonic probe is a function of the observation depth and depends on the geometry of the radiating surface and the radiated wave length.

The aim of the present paper is to indicate the possibilities of decreasing the width of the ultrasonic beam, i.e. to improve the lateral resolution of *B*-mode ultrasonic equipment.

2. Method

The well known method of reducing the diameter of the radiated ultrasonic beam is the use of a lens superimposed on the ultrasonic probe or the use of probes with appropriately profiled concave transducers [1]. This kind of focusing is efficient only over a short depth range. This is a serious disadvantage of this method.

It is possible to focus over the whole observation range when a multi-element ultrasonic probe, controlled by an appropriate electronic system, is used [3, 4, 7]. A multi-element annular ultrasonic probe consists of co-axial elements: a disc and the surrounding rings. The disc and the rings are excited to vibrate by transmitters attached to them. The excitation time of a successive element in the probe is related to the curvature of the radiated ultrasonic wave front, which is focused on the axis of the transducer at a desired distance from its surface (Fig. 1). When the successive elements of the probe are excited to work with various delays, the ultrasonic waves generated by these elements reach at the same time the point P, where summing up they give the effect of the focusing of the ultrasonic beam. At transmission the wave front can be focused only at one depth. When at transmission the ultrasonic beam is to have a small diameter over the whole range of investigation, it is necessary to generate ultrasonic waves of different curvatures of the wave front radiated.

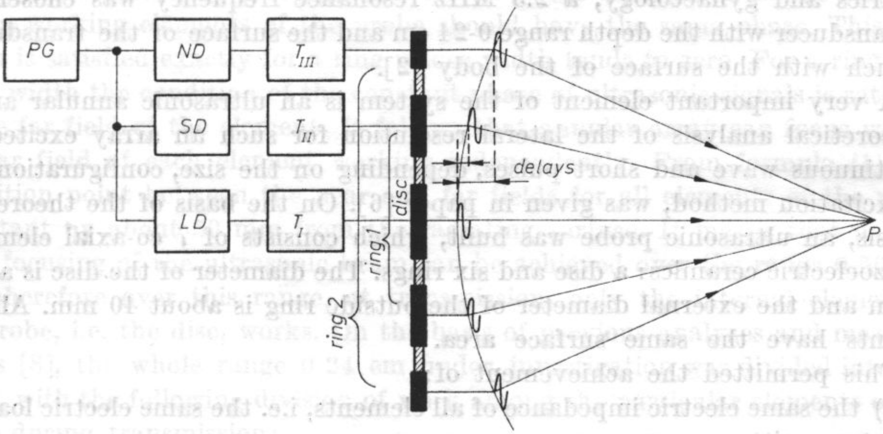

Fig. 1. Focusing during transmission. *PG* — pulse generator, *ND* — transmitter triggering without delay, *SD* — transmitter triggering with small delay, *LD* — transmitter triggering with large delay, *T* — transmitters

This corresponds to several foci over the investigated range. Unlike the focusing at several points during transmission, in the case of detection it is possible to achieve continuous focusing, by a continuous change of the delay of the signals received. The delay changes at a velocity equal to the ultrasonic wave propagation velocity in the body investigated (Fig. 2). This kind of focusing is called dynamic focusing and has a substantial effect on the improvement in the lateral resolution. Focusing using an annular array can be achieved

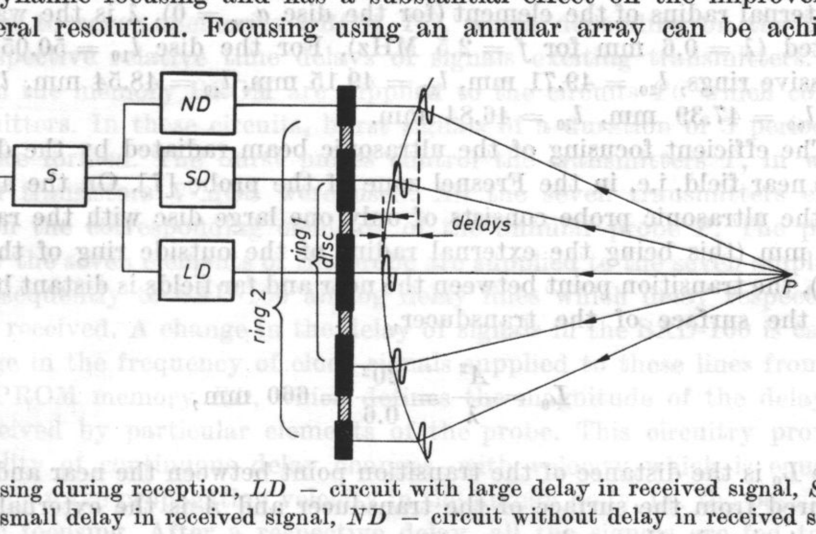

Fig. 2. Focusing during reception, *LD* — circuit with large delay in received signal, *SD* — circuit with small delay in received signal, *ND* — circuit without delay in received signal, *S* — summator

only along the axis of the transducers and therefore, in order to achieve a cross-section of the body investigated, the ultrasonic probe has to be moved mechanically.

In view of the expected use of the ultrasonic beam focusing system in obstetrics and gynaecology, a 2.5 MHz resonance frequency was chosen for the transducer with the depth range 0-24 cm and the surface of the transducers in touch with the surface of the body [2].

A very important element of the system is an ultrasonic annular array. A theoretical analysis of the lateral resolution for such an array excited by a continuous wave and short pulses, depending on the size, configuration and the excitation method, was given in paper [6]. On the basis of the theoretical analysis, an ultrasonic probe was built, which consists of 7 co-axial elements of piezoelectric ceramics: a disc and six rings. The diameter of the disc is about 10 mm and the external diameter of the outside ring is about 40 mm. All the elements have the same surface area.

This permitted the achievement of:

a) the same electric impedance of all elements, i.e. the same electric loading of all transmitters;

b) practically the same distance from the surface of the probe, of the transition point between the near and far fields for the disc and all the rings. This distance is given by formula (1) [7],

$$l_{n0} = \sqrt{\left(\frac{a_{nz}^2}{\lambda} - \frac{a_{nw}^2}{\lambda} - \frac{\lambda}{4}\right)^2 - a_{nw}^2}, \tag{1}$$

where l_{n0} is the distance of the transition point between the near and far fields for each element of the probe, a_{nz} is the external radius of the element, a_{nw} is the internal radius of the element (for the disc $a_{nw} = 0$), λ is the wave length radiated ($\lambda = 0.6$ mm for $f = 2.5$ MHz). For the disc $l_{10} = 50.05$ mm; for successive rings, $l_{20} = 49.71$ mm, $l_{30} = 49.15$ mm, $l_{40} = 48.54$ mm, $l_{50} = 48.27$ mm, $l_{60} = 47.39$ mm, $l_{70} = 46.84$ mm.

The efficient focusing of the ultrasonic beam radiated by the disc occurs in the near field, i.e. in the Fresnel zone of the probe [7]. On the assumption that the ultrasonic probe consists of only one large disc with the radius $A = 20$ mm (this being the external radius of the outside ring of the annular array), the transition point between the near and far fields is distant by 660 mm from the surface of the transducer,

$$L_0 = \frac{A^2}{\lambda} = \frac{20^2}{0.6} = 660 \text{ mm}, \tag{2}$$

where L_0 is the distance of the transition point between the near and far fields measured from the surface of the transducer and A is the external radius of the last ring in the probe.

Relation (2) defines the practical restriction of the range of the system described, with the size of the ultrasonic transducer given previously.

An additional condition for the focusing of the ultrasonic beam by means of the annular array is that signals received at the focus from all the independently working elements of the probe should have the same phase. This condition is satisfied exactly for a ring whose width tends to zero. For a ring with finite width the condition of the constant phase of ultrasonic signals is satisfied in the far field of the element. It follows that annular array can focus well in the far field of each element working independently. From formula (1), the transition point between the near and far fields for all elements of the probe is distant by about 50 mm from the radiating surface. It means that no efficient focusing of the ultrasonic beam can be achieved over the range 0-50 mm and therefore over this range, at transmission, only the internal element of the probe, i.e. the disc, works. On the basis of previous analyses and measurements [8], the whole range 0-24 cm under investigation was divided into five zones, with the following division of work among the particular elements of the probe during transmission:

zone 1: from 0 to 50 mm, with only the disc transmitting;

zone 2: from 50 to 70 mm, with the focus at a distance of 60 mm, three elements: the disc and two internal rings, transmitting;

zone 3: from 70 to 90 mm, with the focus at a distance of 80 mm;

zone 4: from 90 to 140 mm, with the focus at a distance of 110 mm;

zone 5: from 140 to 240 mm, with the focus at a distance of 180 mm.

In zones 3, 4 and 5 all the seven elements of the probe transmit.

The annular array works with an electronic system whose schematic diagram is given in Fig. 3. At transmission, signals from the pulse generator *PG* are supplied to seven memories PROM *TD*, which depending on the focus, set the respective relative time delays of signals exciting transmitters. The pulses from the memory PROM are supplied to the circuits *TC* which control the transmitters. In these circuits, burst signals of a duration of 3 periods of 2.5 MHz are formed. The burst pulses control the transmitters *T*, in which fast switch transistors V-MOS were used. All the seven transmitters excite to vibration the corresponding elements of the annular probe *P*. The pulses received by the seven elements of the probe are supplied to the seven amplifiers *R* and subsequently to SAD-100 analog delay lines which delay respectively the signals received. A change in the delay of signals in the SAD-100 is caused by a change in the frequency of clock signals supplied to these lines from the very fast PROM memory *RD*, which defines the magnitude of the delays of signals received by particular elements of the probe. This circuitry provides the possibility of continuous delay changes, with velocity which is equal to the ultrasonic wave propagation velocity in the human body, i.e. the possibility of dynamic focusing. After a respective delay, all the signals are fed to the summator *S*, where they are summed up. Since the SAD-100 delay lines work using the signal sampling principle, it is necessary to filtrate signals at the sampling frequency. This is achieved by the filter F following the summator.

3. Calculation of the distribution of the radiated acoustic field

This problem consists in the calculation of the space and time distribution of the acoustic field generated by the radiating surfaces of the multi-element ultrasonic annular array. These surfaces are excited to vibration by signals

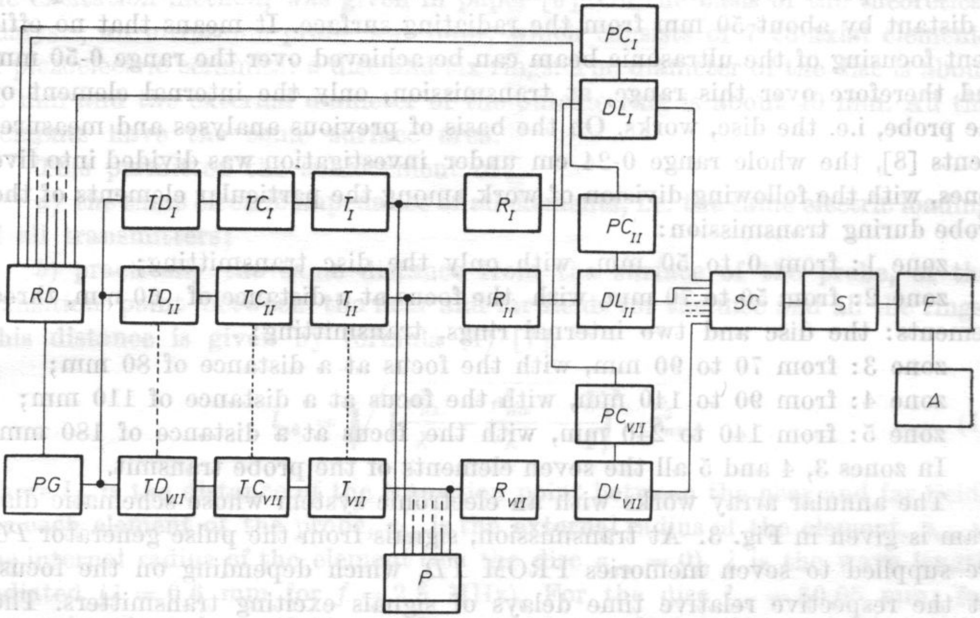

Fig. 3. A schematic diagram of the electronic system working with an annular array. PG — pulse generator, TD — PROM memories of the transmitted pulse delay, TC — transmitter control, T — transmitters, P — probe, R — receivers, DL — SAD-100 delay lines, RD — PROM memory (change in the received signal delay), PC — pulse control of the SAD-100 delay lines, SC — switch circuitry, S — summator, F — filter, A — amplifier

in the form of high-frequency pulses with delays so selected that the beam focuses at a desired point of the field. In the calculations, a pulse shape closest to one in practice was assumed. This pulse contains five sinusoidal high-frequency periods with the envelope $\sin^2(\pi t/2)$.

The theoretical method for the calculation of the acoustic field is based on analysis of transient fields generated by piston surfaces. This analysis consists in the determination of the pulse response of a radiating surface at a given point in space and subsequently in the convolution of this response with the exciting pulses.

The problem of the analytical determination of the distribution of the acoustic field as a function of time, at any point in a half-space, generated by the vibrating surface of an annular array, was considered in paper [5]. According to the formulae derived in this paper, analytical expressions for the calculation of the time behaviour of acoustic pressure, focused on the axis at the distance z from the radiating surface, become

$$P_{\Sigma}(\boldsymbol{r}, t) = P_0(\boldsymbol{r}, t) + \sum_{N} P_n(\boldsymbol{r}, t), \tag{3}$$

where $P_0(\boldsymbol{r}, t)$ is the time behaviour of the acoustic pressure generated by the central disc, $P_n(\boldsymbol{r}, t) = P_{nz}(\boldsymbol{r}, t) - P_{nw}(\boldsymbol{r}, t)$ is the time behaviour of the acoustic pressure generated by the nth ring with the external radius a_{nz} and the internal radius a_{nw};

$$P_{\Sigma}(\boldsymbol{r}, t) = \varrho\{\dot{h}_0(\boldsymbol{r}, t) * V_0(t) + \sum_{N} [\dot{h}_{nz}(\boldsymbol{r}, t) * V_n(t) - \dot{h}_{nw}(\boldsymbol{r}, t) * V_n(t)]\}, \tag{4}$$

where ϱ is the density of the medium, t is time, $\boldsymbol{r}$ is the vector of the distance between a point source and the observation point in the half-space, $V_0(t) = V[H(t) - H(t-\tau_0)]\sin^2(\pi t/2)\sin\omega t$ is the vibration velocity of the central disc, $V_n(t) = V[H(t-\Delta\tau_n) - H(t-\Delta\tau_n-\tau_0)]\sin^2[\pi/2(t-\Delta\tau_n)]\sin\omega(t-\Delta\tau_n)$ is the vibration velocity of the nth ring, $\Delta\tau_n$ is the time difference (acceleration) in the excitation of the nth ring with respect to the disc; $\dot{h}_0(\boldsymbol{r}, t)$, $\dot{h}_{nz}(\boldsymbol{r}, t)$ and $\dot{h}_{nw}(\boldsymbol{r}, t)$ are respectively the partial derivatives with respect to time of the pulse responses for the central disc and rings with the radii a_{nz} and a_{nw}.

The calculations were taken on a VAX computer at Limburg University (the Netherlands) in Fortran. From these calculations, the width of the ultrasonic beam was determined over the whole range for signal level decreases of respectively 3 dB, 6 dB and 10 dB. The 3 dB and 6 dB and 10 dB beam – widths determined analytically are shown in Fig. 15 (section 5) in the form of dotted curves, together with the experimental results.

4. Measurement methods

The measurements were taken on the acoustic pressure of the ultrasonic field of the annular array at transmission. The measurement conditions were the following:

zone 1: pulses transmitted only by the disc;

zone 2: pulses transmitted by three elements; disc and two internal rings;

zones 3, 4 and 5: pulses transmitted by all the elements of the probe.

All the elements of the probe were excited to vibration by a burst with a duration of three cycles of the 2.5 MHz signal. A hydrophone of piezoelectric pvdf (polyvinylidene fluoride) foil (with the diameter of the active part being

1 mm, the thickness 25 mm), manufactured by Marconi (Fig. 4), with a known directional response, was used as the measurement element. This hydrophone is characterized by a flat response of signals received as a function of frequency

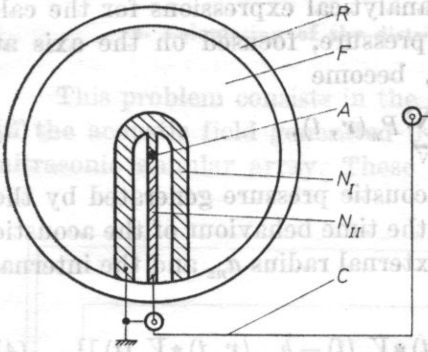

Fig. 4. The hydrophone of pvdf foil manufactured by Marconi, R — frame, F — pvdf foil, N_I — part of the upper foil surface covered with a gold layer, N_{II} — part of the lower foil surface covered with a gold layer, A — active region where the gold-covered parts of the upper and lower surfaces overlap, C — concentric cable

over the range 1-10 MHz and by its lack of effect on the distribution of the ultrasonic field at the measurement point.

As a confirmation of the validity of the parameters assumed for the exciting pulse in the calculation of the field distribution, Fig. 5 shows a pulse shape detected by the pvdf hydrophone at transmission by the disc. The signal detected

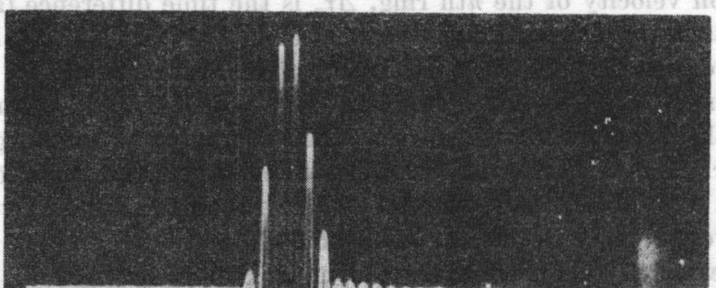

Fig. 5. The pulse shape received by the hydrophone at transmission by the disc

contains about five 2.5 MHz cycles modulated by a signal of the approximate shape $\sin^2(\pi t/2)$ of 2 μs duration.

The acoustic pressure distribution was measured by the system shown in Fig. 6. Ultrasonic waves radiated by particular elements of the array P are received by the hydrophone H, transformed into electric pulses and fed to the amplifier A. After amplification the signals are fed to the oscilloscope O. The hydrophone can be moved in the direction x and y, with high shifting accuracy. On account of the symmetry of the system, measurements were

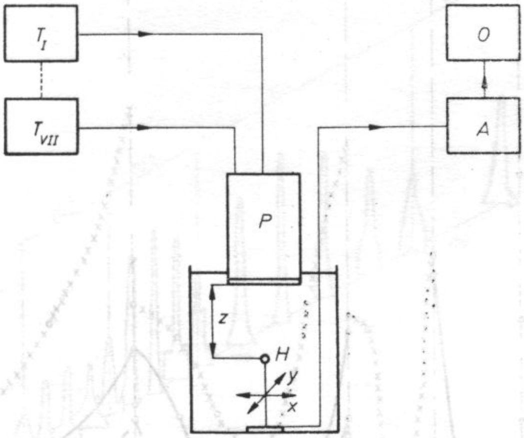

Fig. 6. The system for the measurement of the acoustic pressure. T — transmitters, P — probe, H — hydrophone, A — amplifier, O — oscilloscope, z — probe-hydrophone distance, x, y — directions of the hydrophone shift

taken only for a shift in one direction from the axis of the system. With individual work of each element of the probe, signals detected by the hydrophone were adjusted for the distance $z = 110$ mm (the focus of zone 4). The measured results are shown in Fig. 7.

Zone 1 is in the near field of the element and therefore measurements were taken only for two probe-hydrophone distances, 40 mm and 50 mm. For zones closer to the probe, 2 and 3, "point focusing", i.e. good focusing at the focus and worse at the ends of the zone, can distinctly be seen.

For farther zones, 4 and 5, slightly worse focusing can be seen at points close to the focus, at the expense of the more uniform focusing over the whole zone. For comparison, a half beamwidth is shown for respective 3 dB, 6 dB, 10 dB and 20 dB decreases in signal level. The determination of the 3 dB beamwidth does not take into account the effect of the side lobes. The determination of the 20 dB beamwidth is also inconvenient because of the overlarge effect of the side lobes on the response, e.g. in the case of the 20 dB beamwidth in zone 2. With focussing at transmission only, it is best to determine the beamwidth at a level of — 6 dB or — 10 dB. In addition, when focusing at the same points at reception, the curves for — 6 dB and — 10 dB (Fig. 7) define the respective beamwidths at signal level decreases to 12 dB and 20 dB with focusing both at transmission and detection. This is satisfied under the condition that the directional patterns are the same both at transmission and reception.

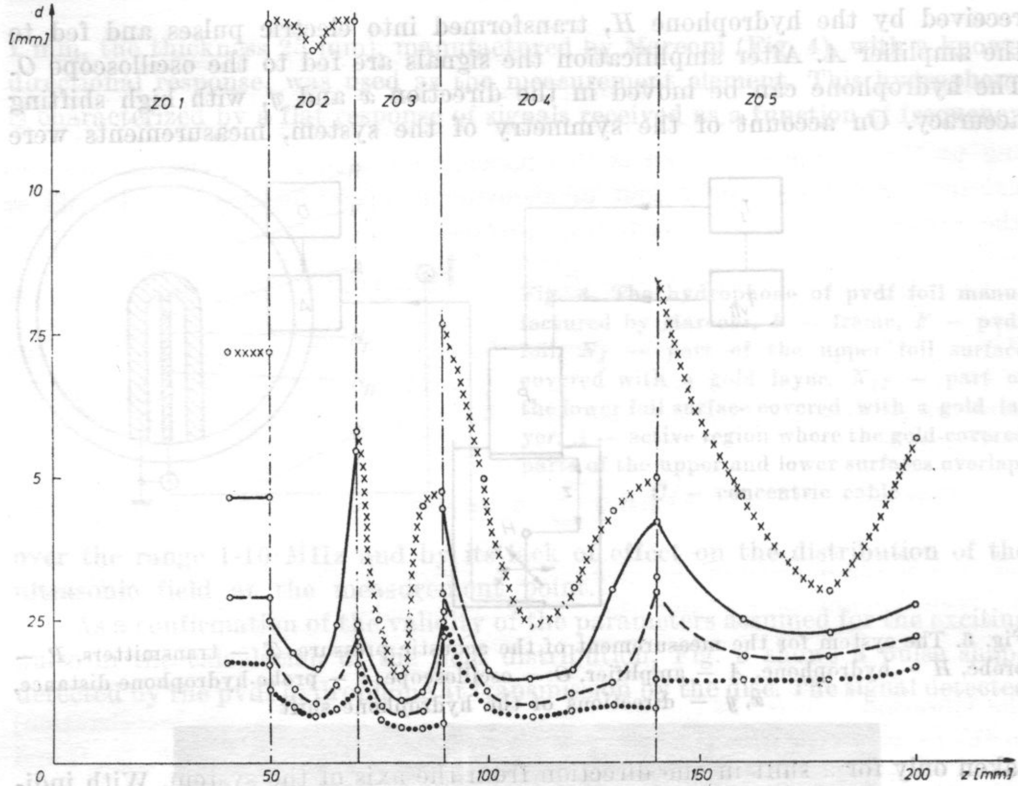

Fig. 7. Half beamwidth for different values of the drop in the signal received, d — half beamwidth, z — distance from the probe, ZO — zone division of the range, ... 3 dB half beamwidth, — — — 6 dB half beamwidth, —·—· 10 dB half beamwidth, xxx 20 dB half beamwidth, 000 — measurement points

At reception the described system implements dynamic focusing, for which, over the whole zone under study, ultrasonic signals reflected from points on the axis of the system are focused.

The combination of dynamic focusing at reception with focusing in several zones at transmission causes a decrease in the ultrasonic beamwidth, with respect to focusing in zones both at transmission and detection. The improvement is particularly distinct at the ends of zones.

Fig. 8 shows the distribution of signal amplitudes over the whole range. Greater amplitudes occur in zones 3, 4 and 5; it should be mentioned, however, that all the elements transmit to these zones. At the ends of zones 2 and 3 there is a distinct effect of the side lobes. It can be seen from the plots in the figure that the amplitude distribution is rather regular over the whole range under study.

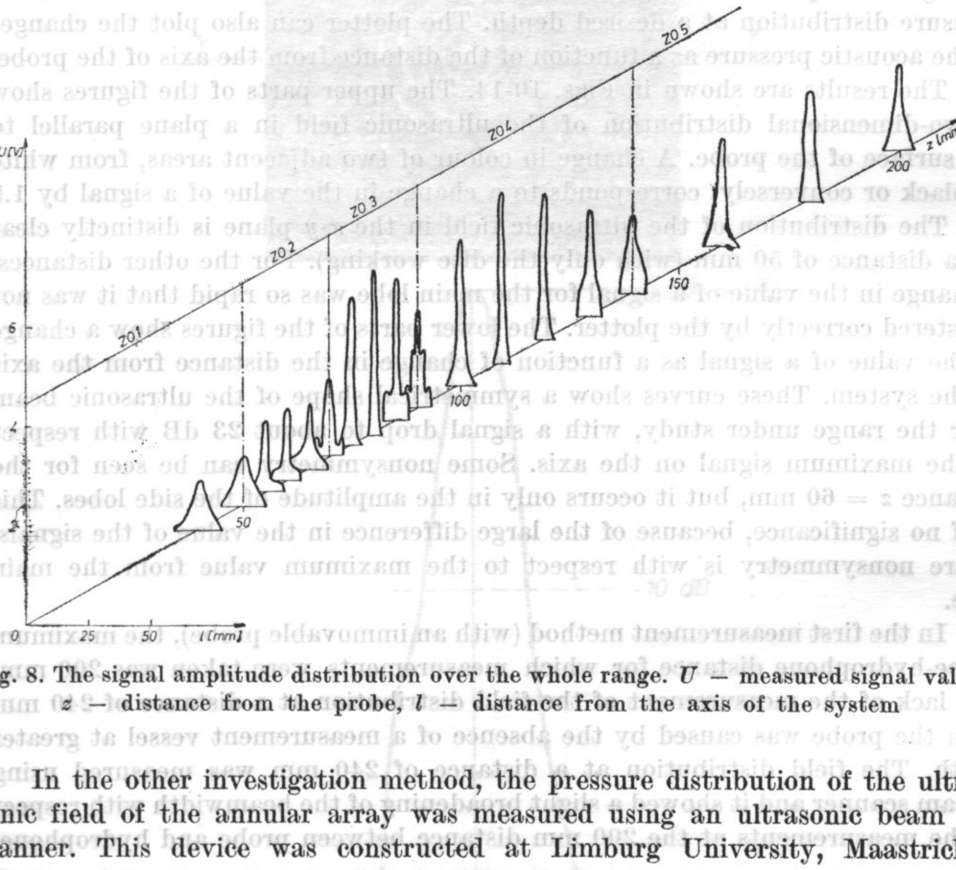

Fig. 8. The signal amplitude distribution over the whole range. U — measured signal value, z — distance from the probe, l — distance from the axis of the system

In the other investigation method, the pressure distribution of the ultrasonic field of the annular array was measured using an ultrasonic beam — scanner. This device was constructed at Limburg University, Maastricht. Fig. 9 explains the principle of work of this device. In this case the hydrophone

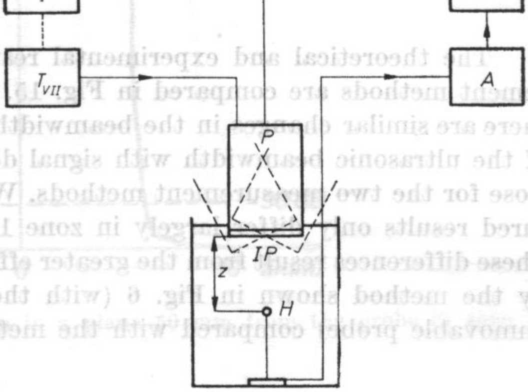

Fig. 9. The working principle of the beam scanner. T — transmitters, P — probe, H — hydrophone, A — amplifier, $X-Y$ — $x-y$ plotter, z — probe — hydrophone distance, IP — immovable point on the surface of the probe, round which the probe swings

is immovable and set on the axis of the system. The ultrasonic probe swings in all directions round the point *IP* which lies both on the axis of the system and on the surface of the transducer. Signals from the hydrophone are fed through an amplifier to a *x-y* plotter, which can plot a two-dimensional acoustic pressure distribution at a desired depth. The plotter can also plot the changes in the acoustic pressure as a function of the distance from the axis of the probe.

The results are shown in Figs. 10-14. The upper parts of the figures show a two-dimensional distribution of the ultrasonic field in a plane parallel to the surface of the probe. A change in colour of two adjacent areas, from white to black or conversely, corresponds to a change in the value of a signal by 1.5 dB. The distribution of the ultrasonic field in the *x-y* plane is distinctly clear for a distance of 50 mm (with only the disc working). For the other distances, a change in the value of a signal for the main lobe was so rapid that it was not registered correctly by the plotter. The lower parts of the figures show a change in the value of a signal as a function of change in the distance from the axis of the system. These curves show a symmetrical shape of the ultrasonic beam over the range under study, with a signal drop to about 23 dB with respect to the maximum signal on the axis. Some nonsymmetry can be seen for the distance $z = 60$ mm, but it occurs only in the amplitude of the side lobes. This is of no significance, because of the large difference in the value of the signals, where nonsymmetry is with respect to the maximum value from the main lobe.

In the first measurement method (with an immovable probe), the maximum probe-hydrophone distance for which measurements were taken was 200 mm. The lack of the measurement of the field distribution at a distance of 240 mm from the probe was caused by the absence of a measurement vessel at greater depth. The field distribution at a distance of 240 mm was measured using a beam scanner and it showed a slight broadening of the beamwidth with respect to the measurements at the 200 mm distance between probe and hydrophone.

5. Comparison of theoretical and experimental results

The theoretical and experimental results obtained using the two measurement methods are compared in Fig. 15. It can be seen that in all the cases there are similar changes in the beamwidth shape. The results of measurements of the ultrasonic beamwidth with signal decreases of 3 dB and 6 dB are very close for the two measurement methods. With a signal drop of 10 dB the measured results only differ largely in zone 1 and at the ends of zones 2 and 3. These differences result from the greater effect of the side lobes in measurements by the method shown in Fig. 6 (with the hydrophone being shifted and an immovable probe) compared with the method using the beam scanner.

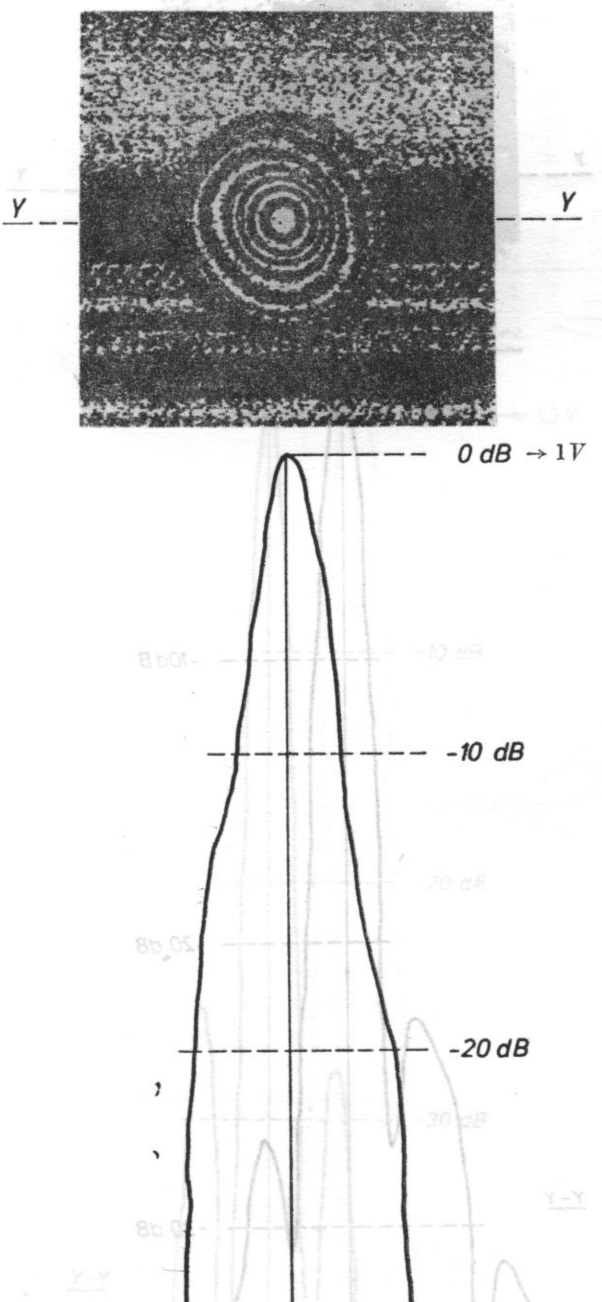

Fig. 10. The ultrasonic field distribution in a plane 50 mm from the probe in zone I

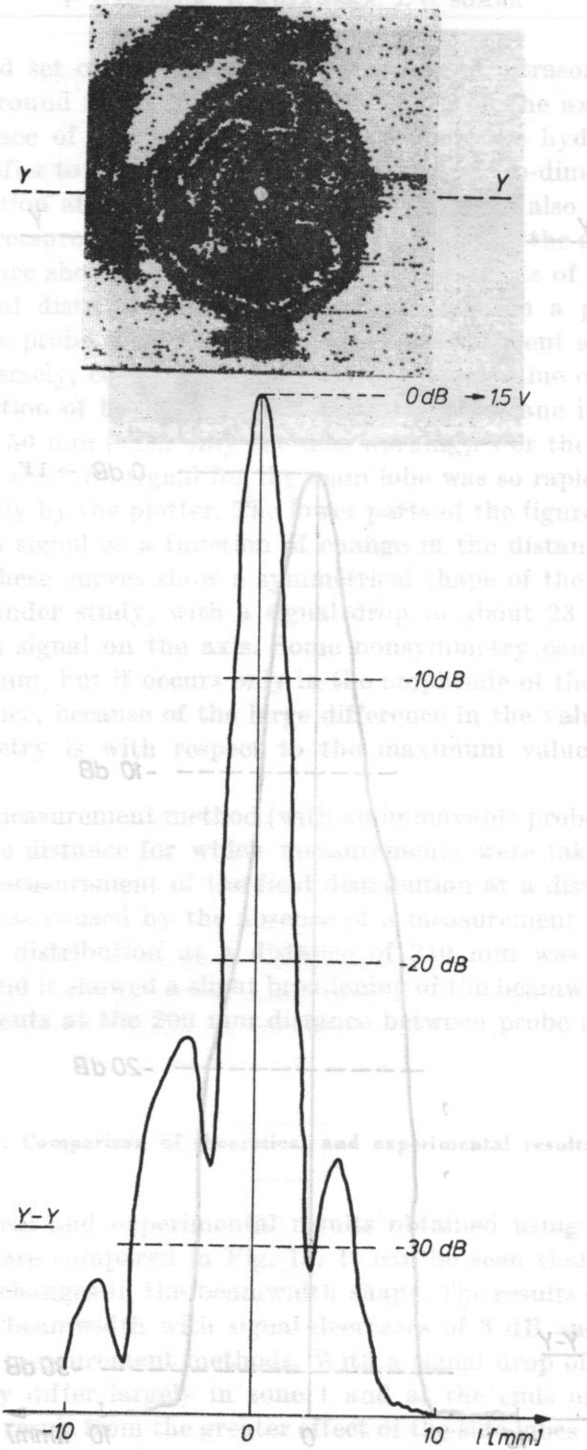

Fig. 11. The ultrasonic field distribution in a plane 60 mm from the probe in zone 2

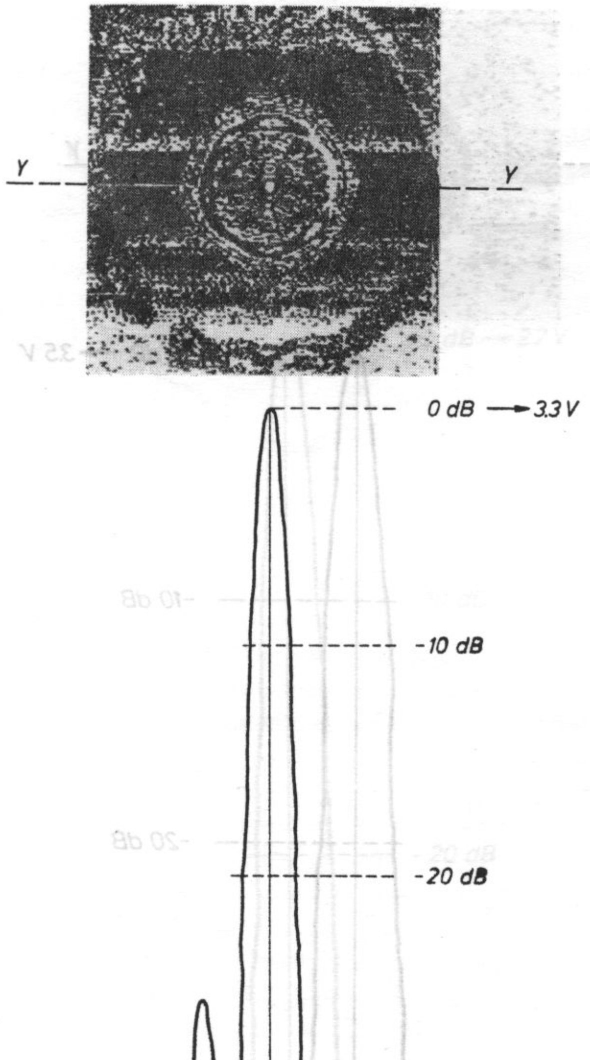

Fig. 12. The ultrasonic field distribution in a plane 80 mm from the probe in zone 3

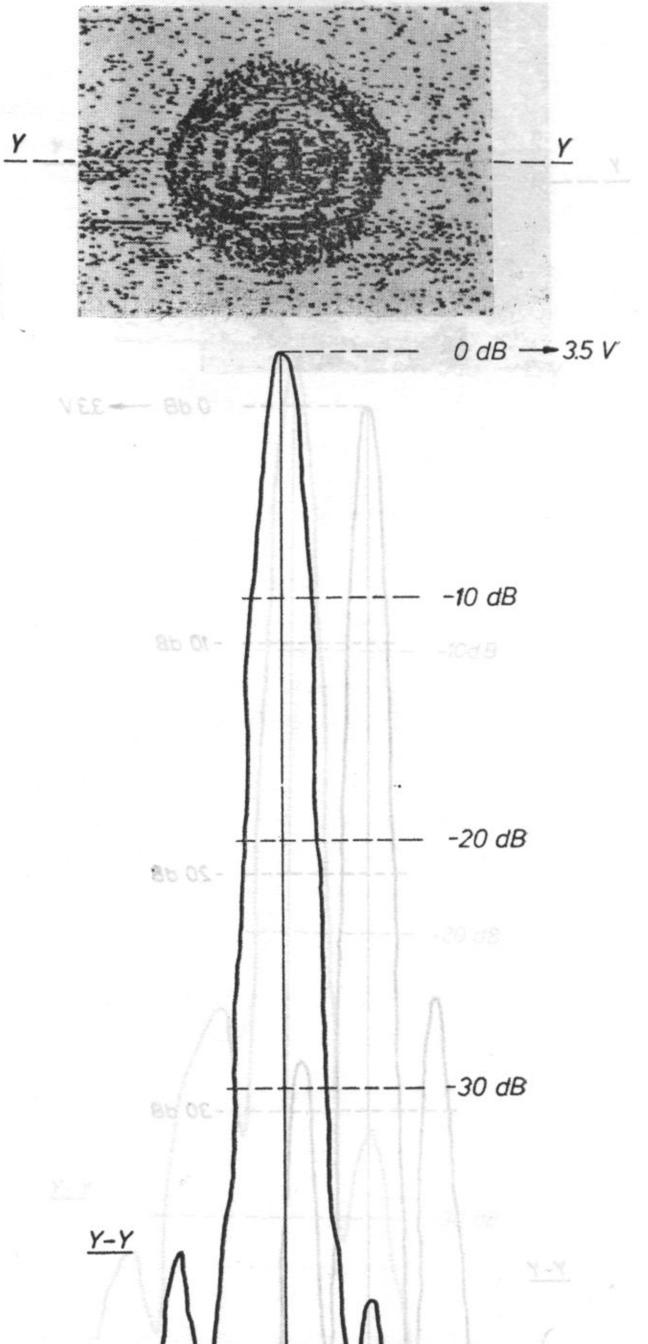

Fig. 13. The ultrasonic field distribution in a plane 110 mm from the probe in zone 4

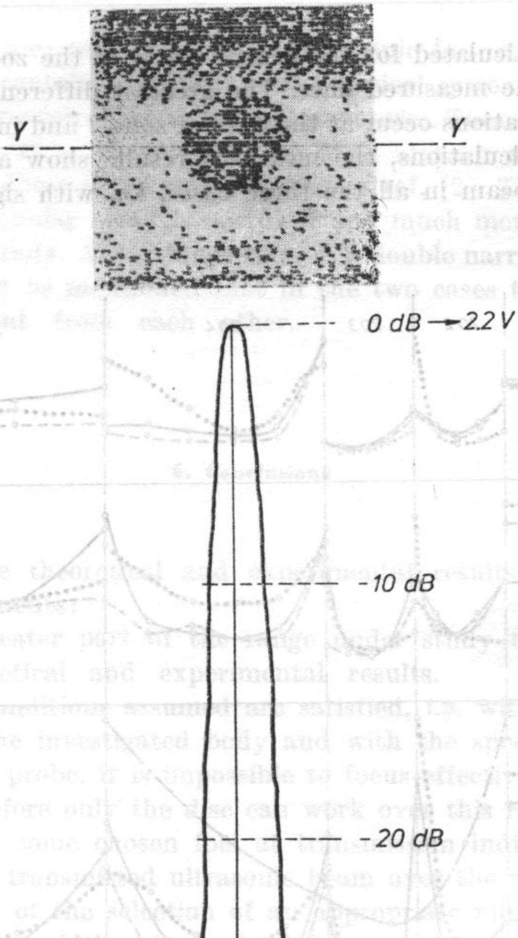

Fig. 14. The ultrasonic field distribution in a plane 180 mm from the probe in zone 5

The results calculated for the central parts of the zones are generally in agreement with the measured ones. The greatest differences between measurements and calculations occur at the ends of zone 2 and in zone 4. When compared with the calculations, the measured results show a slightly less width of the ultrasonic beam in all the three cases, i.e. with signal drops of 3 dB, 6 dB and 10 dB.

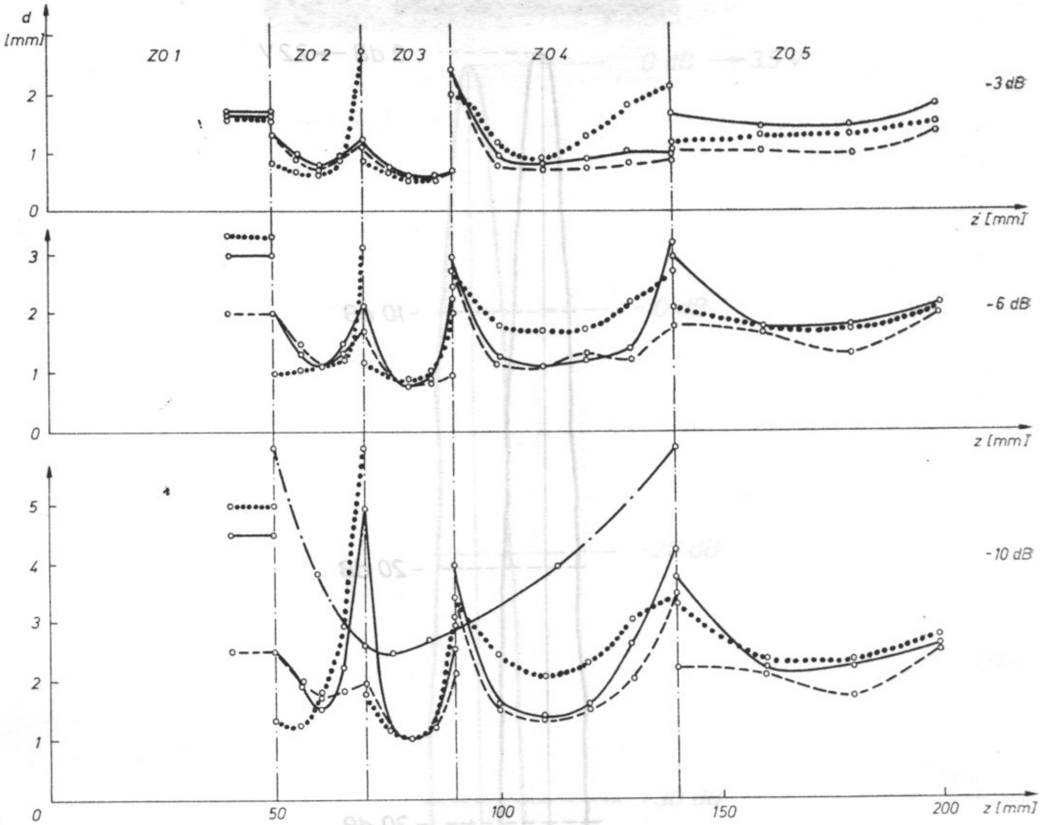

Fig. 15. Comparison of the theoretical and experimental results for signal drops of 3 dB, 6 dB and 10 dB. d – half beamwidth, z – distance from the probe, ZO – zone division of the range, – measurements (shifted hydrophone), – – – measurements (swinging probe), . . . calculations, –.–.–.– typical system used in the ultrasonograph for investigation of the abdominal structures: $f = 2.5$ MHz, $\varphi = 20$ mm; ooo – measurement points

From the measurements taken, it was found that in the two measurement methods the side lobes are at the same distance from the axis. In measurements by the beam scanner the amplitude of the side lobe with respect to the main lobe is less than in the method using a shifted hydrophone. For calculations in zones 2, 3 and 4 the side lobes are slightly closer to the axis than in the experimental results.

The results of measurements of the ultrasonic beamwidth with a signal drop of 10 dB also contain the response of a typical system used in the ultrasonograph for examination of the abdominal structures. These data were obtained from measurements at a frequency of 2.5 MHz and for an ultrasonic beam radiated by a transducer of 20 mm diameter in ref. [2]. The ultrasonic beam generated by the annular array is narrower and much more regular over the whole range under study. At the focus there is a double narrowing of the beamwidth, but it should be mentioned that in the two cases the transducer diameters are different from each other.

6. Conclusions

Analysis of the theoretical and experimental results obtained permits the following statements:

1. Over the greater part of the range under study there is agreement between the theoretical and experimental results.

2. When the conditions assumed are satisfied, i.e. with a direct contact to the surface of the investigated body and with the specific dimensions of the elements of the probe, it is impossible to focus effectively over the range 0-50 mm, and therefore only the disc can work over this range.

3. Focusing for some chosen foci at transmission indicates a narrowing of the width of the transmitted ultrasonic beam over the range under study, under the condition of the selection of an appropriate number of these foci. In view of a large beamwidth at the ends of the zones, with respect to the beamwidth at the focus, it seems, from the results obtained, to be purposeful to increase the number of the zones from five to seven or eight.

4. Focusing for some chosen foci only at transmission can sometimes be useful in practice, particularly because of the simplicity of the electronic systems employed.

5. In addition, when using dynamic focusing at reception, there is an optimum narrowing of the beam at all distances, i.e. an improvement in the lateral resolution of the ultrasonograph investigation of the internal structures of the body.

Acknowledgement. The authors wish to thank Prof. Dr. L. Filipczyński (Institute of Fundamental Technological Research, Polish Academy of Sciences, Warsaw) and Dr. A. Hoeks (Limburg University, Maastricht, Holland) for discussion and valuable suggestions in the course of the preparation of this paper.

References

[1] L. Filipczyński, G. Łypacewicz, J. Sałkowski, T. Waszczuk, *Automatic eye vizualization and ultrasonic intensity determination in focused beams by means of electrodynamic and capacitance methods*, Ultrasonics in Medicine, ed. Katzner *et al.*, Excerpta Medica, Amsterdam – Oxford 1975.

[2] L. Filipczyński, I. Roszkowski, *Ultrasonic diagnosis in obstetrics and gynaecology* (in Polish), PZWL, Warsaw 1977.

[3] M. Hubelbank, O. J. Tretiak, *Focused ultrasonic transducer design*, M. I. T. Res. Lab. Elec. Q. P. R. 1971, 169-177 (1971).

[4] G. Kossoff *et al.*, *Annular phased arrays in ultrasonic obstetrical examinations*, Advanced Study Institute, Ultrasonic Diagnostics, Milan, June 1974.

[5] T. Kujawska, *Dynamic focusing of an ultrasonic beam by a phased array using the pulse method*, Archives of Acoustics (in press).

[6] T. Maruk-Kujawska, *Dynamic focusing of an ultrasonic beam by annular transducers* (in Polish), doct. diss., Institute of Fundamental Technological Research, Polish Academy of Sciences, Warsaw 1980.

[7] H. E. Melton, F. L. Thurstone, *Annular array design and logarithmic processing for ultrasonic imaging*, Ultrasound in Biology and Medicine, 4, 1-12 (1978).

[8] T. Waszczuk, J. Somer, *System for dynamic focusing of an ultrasonic beam using annular array, practical implementation*, Proc. XXVII Open Seminar on Acoustics, Warsaw – Puławy, September 1980.

Received on 10 March, 1983.